Cellulose (2015) 22:1565–1576
DOI 10.1007/s10570-015-0619-x

ORIGINAL PAPER

Impact of mechanical and enzymatic pretreatments on softwood pulp fiber wall structure studied with NMR spectroscopy and X-ray scattering

Tommi Virtanen · Paavo A. Penttilä · Thaddeus C. Maloney · Stina Grönqvist · Taina Kamppuri · Marianna Vehviläinen · Ritva Serimaa · Sirkka Liisa Maunu

Received: 13 October 2014 / Accepted: 30 March 2015 / Published online: 12 April 2015

Abstract Dissolution of wood pulp can be enhanced by applying certain pretreatments before exposing the fibers to solvents. We have analyzed effect of mechanical and enzymatic pretreatments on softwood fiber wall structure using nuclear magnetic resonance (NMR) spectroscopic methods, small and wide angle X-ray scattering (SAXS, WAXS). NMR diffusometry was used to estimate the effect of pretreatments on average pore sizes at micrometer size scale and for the connectivity of the porous network. A proton NMR experiment was used to quantify the nonfreezing water content inside the fiber wall, and solid state NMR ^{13}C cross polarization (CP) magic angle spinning (MAS) spectroscopy was used to observe the effect of pretreatments on crystallinity and lateral fibril dimensions of cellulose fibrils, and in combination with fiber saturation point measurement to calculate the average pore size at nanometer size scale. Both WAXS and CP–MAS NMR experiments confirmed that there were no changes in crystallinity nor in fibril lateral dimensions due to pretreatments. The pretreatments caused an increase in the amount of nonfreezing water, suggesting an opening of the pore system. According to diffusion experiments there are only minor changes in micrometer scale pore network due to pretreatments. SAXS results indicated that enzymatic treatment increased the microfibrillar distance, and there was also an increase in cross relaxation rate of magnetization from water to cellulose protons as observed by NMR. These were interpreted to be due to opening of microfibrillar bundles, leading to an increased accessibility of water.

Keywords Softwood pulp · NMR spectroscopy · Diffusion · Enzymatic hydrolysis · SAXS · WAXS

T. Virtanen (✉) · S. L. Maunu
Laboratory of Polymer Chemistry, University of Helsinki, P.O. Box 55, 00014 Helsinki, Finland
e-mail: tommi.virtanen@helsinki.fi

P. A. Penttilä · R. Serimaa
Department of Physics, University of Helsinki, P.O. Box 64, 00014 Helsinki, Finland

T. C. Maloney
Aalto University School of Chemical Technology, P.O. Box 16300, 00076 Aalto, Finland

S. Grönqvist
Technical Research Centre of Finland (VTT), P.O. Box 1000 (TT2), 02044 Espoo, Finland

T. Kamppuri · M. Vehviläinen
Fibre Materials Science, Tampere University of Technology, P.O. Box 589, 33101 Tampere, Finland

Introduction

Cellulose, with seemingly endless resources, is a tempting material for various industrial fields when they seek solutions that take advantage on renewable biological materials. Yet, its utilization has not

reached its full potential, at least partially due to difficulties in getting cellulose in dissolved state (Zhu et al. 2006). Wood pulping is the most common way to produce almost pure cellulose, and it would therefore be beneficial to be able to directly dissolve wood pulp. This is, however, complicated by remnant cell wall structures and supramolecular long-range arrangements of cellulose fibrils in fibers (Cuissinat and Navard 2006; Moigne and Navard 2010) that slow down the dissolution process, and may lead to incomplete dissolution. Direct dissolution of wood pulp can be enhanced by applying pretreatments prior the actual dissolution step in order to increase the reactivity of the cellulose fibrils towards solvent chemicals, and to weaken the cell wall structures (Ibarra et al. 2010; Moigne et al. 2010; Kihlman et al. 2011; Ambjörnsson et al. 2013). Cost efficient, straight forward methods to bring cellulose from pulp fibers into solution state are a prerequisite for industrial scale applications.

One of the factors affecting the dissolution properties is the pore system of the fiber, as it is related to the capability of solvent chemicals to access the interiors of the fiber (Engström et al. 2006). As the pore structure of pulp also has an influence on the papermaking properties (Andreasson et al. 2003), it has been earlier studied extensively with numerous methods, like thermoporosimetry (Maloney et al. 1998; Wang et al. 2006), cryoporometry (Östlund et al. 2010), and nuclear magnetic resonance (NMR) diffusometry (Topgaard and Söderman 2002a). The size scale of the pores sets the limit for molecules that can penetrate the fiber wall, and both size of the pores and their connectivity may be a factor in determining the rate of dissolution. Pores are partially created by pulping process: As non-cellulosic components are removed, they leave cavities that become filled with water (Maloney and Paulapuro 1999). The size distribution of the pore system extends from a few nanometers up to micrometer lengths (Persson et al. 2004), and it is dependent on the moisture content of the pulp: especially the macropores created during pulping tend to close when water is removed. The pores smaller than 2.5 nm are more inert for changes in moisture content (Pönni et al. 2012). During pulping the removal of hemicelluloses and lignin, together with elevated temperature, causes also an increase in cellulose fibril aggregate dimensions (Hult et al. 2001; Fahlén and Salmén 2005). It is assumed that the enlargement of the aggregates is accompanied by a formation of microfibrillar bridges between adjacent aggregates (Fahlén and Salmén 2003). Upon fiber drying there is a further increase in lateral fibril aggregate dimension (Chunilall et al. 2010), this leads to loss of swelling capacity that can not be fully recovered by rewetting the fiber.

Our purpose in this work was to characterize the effects of mechanical pretreatment and subsequent enzymatic hydrolysis to the soft wood dissolving grade pulp fiber wall structure, with a partial interest in seeing the effect of pre-drying of the pulp. Mechanical treatment was performed by shredding (Baker Perkins), with length of the treatment being one factor. The pulp sample with longest shredding time was subsequently enzymatically hydrolyzed using a commercial endoglucanase. It has been earlier found that applying a 300 min shredding by Baker Perkins mixer and subsequent endoglucanase treatment modifies dissolving grade fibers to become soluble into NaOH/ZnO solvent system (Vehviläinen et al. 2009). The effect of the Baker Perkins shredding in combination with enzymatic hydrolysis on pulp dissolution was also recently studied by Parviainen et al. (2014) with optical microscopy and differential scanning calorimetry. In their work selected ionic liquids were used to dissolve the pulp samples, and according to their results the combined pretreatments (mechanical treatment followed by enzymatic hydrolysis) lead to different dissolution behavior than mechanical treatment alone. In this work changes in the fiber wall structure were characterized by means of wide and small angle X-ray scattering (WAXS, SAXS), solid state NMR, and NMR diffusometry. A benefit of NMR spectroscopy is its ability to provide information from various size scales: structures from nanometer scale up to micrometer size scale can be studied depending on choice of experimental method. While solid state ^{13}C cross polarization (CP) magic angle spinning (MAS) NMR is capable of providing information from nanometer scale structures, NMR diffusometry data gives information from micrometer scale pore structures. NMR diffusometry is a form of NMR spectroscopy where motion of the selected molecular species is monitored by labeling their positions utilizing pulsed field gradients (PFG) (Stejskal and Tanner 1965; Johnson 1999), and the self-diffusion

coefficient of the molecular species can be obtained from the intensity reduction caused by PFG. When molecular species are located inside a confined region, like fiber wall pores, their observed diffusion coefficient in a NMR diffusometry experiment deviates from that of freely diffusing species (Woessner 1963). This so called apparent diffusion coefficient is a function of experimentally set diffusion time, and the actual nature of this dependence is governed by the shape and sizes of the pore system (Valiullin and Skirda 2001). Therefore, by determining the diffusion coefficient as a function of diffusion time it is possible to obtain information about average pore sizes and long-range connectivity of the porous network. In this work we used water as a molecular probe, and diffusion experiments were carried out in a wetted state below the freezing temperature of bulk water so that only the water that is enclosed inside the pores and having therefore a depressed freezing point, would contribute to the observed signal (Topgaard and Söderman 2002c). Additionally, we used a proton NMR experiment to quantify the amount of this nonfreezing water (NFW) (Hartley et al. 1994). To account the effect of cross relaxation of magnetization between water and cellulose matrix Goldman–Shen (GS) experiments (Goldman and Shen 1966) were carried out at each measuring temperature. The anisotropy of water diffusion inside the fiber wall was addressed by using a diffusion coefficient distribution in diffusion data analysis.

Experimental

Materials

A commercial spruce–pine dissolving sulphite pulp (cellulose content 89.9 %, viscosity 520 ml/g), obtained as dried sheets, was provided by Domsjö Fabriker Sweden. Mechanical and enzymatic pretreatments were carried out at Tampere University of Technology (TUT) and at Finnish Technological Research Center (VTT).

The pre-wetted pulp was mechanically shredded with a Baker Perkins mixer with two vertical z-shaped shafts, rotating in opposite directions with velocities of 60 and 32 rpm (size 6–1 BB Universal mixer S/N 44777), at a cellulose concentration of 20 % (w/w) for 30–300 min at ambient temperature. Prior to shredding the pre-wetted pulp was gently stirred at 5 % consistency to homogenize it. The enzyme treatments were carried out at pH 5, 50 °C at a pulp consistency of 5 % (w/w) for 30–120 min. The enzyme dosage was 0.25 or 1 mg protein/g fibre. The enzymatic reaction was stopped by heating the pulp to >90 °C and by keeping the temperature for 15 min. After the enzymatic treatments the pulps were filtrated and washed with water. The enzyme used in enzymatic treatments was a commercial endoglucanase rich enzyme preparation (Fibercare R, Novozym CGP20048). The major cellulolytic activity of the enzyme preparation (pH 5, HEC 2764 nkat/ml) was assayed using a standard method (IUPAC 1987). The xylanase activity (pH 5, 4 nkat/ml) was analysed as described by Bailey et al. (1992). The protein content of the enzyme preparation was 15.7 g/l, as analysed by the method of Lowry et al. (1951) using bovine serum albumin as a standard. Studied samples with sample codes and corresponding treatments are listed in Table 1. Chemical characterizations of the studied samples have been carried out in a work by Grönqvist et al. (2014). Dissolution studies for mechanically treated sample, and for sample with combined mechanical and enzymatic treatments were performed by Parviainen et al. (2014).

Table 1 Description of the studied samples

Sample code	Description
REF	No pretreatments
M30	30 min
M60	60 min
M150	150 min
M300	300 min
M300ELD	300 min + E_{LD}[a]
M300EHD	300 min + E_{HD}[b]
ELD	Reference + E_{LD}[a]

Time given in description column is the shredding time. E_{LD} and E_{HD} refer to low and high dosage enzymatic treatments

[a] 0.25 mg/g enzyme dosage

[b] 1.0 mg/g enzyme dosage

WAXS and SAXS

SAXS was measured from samples without drying, thus having a dry matter content of about 25–30 % as measured by weight loss after drying at 105 °C.

WAXS was measured from samples dried in room air. The samples were pressed in metal rings of thickness 1 mm and the wet samples for SAXS were sealed with Mylar foil. The experimental setup for SAXS and WAXS experiments, data treatment, and the curve fitting procedures used to obtain the cellulose crystal size and crystallinity from the WAXS data are described by Penttilä et al. (2013). In short, Gaussian functions corresponding to the diffraction peaks originating from crystalline cellulose were fitted to the data together with an amorphous background (sulphate lignin). Crystallinity was computed based on the ratio of the integrated amorphous background and the total intensity. Crystal size was obtained using the Scherrer equation. In the SAXS analysis, the measured q range was from 0.024 to 0.35 $Å^{-1}$ with the magnitude of the scattering vector $q = 4\pi \sin\theta/\lambda$ and θ half of the scattering angle. The peak location was determined from the $\log(q^2 I)$ versus q plot (Kratky plot) using a parabola fit on the top of the peak.

NMR experiments

All NMR spectra were measured using Bruker Avance III 500 spectrometer with a magnetic flux density of 11.7 T, using a double resonance BB(^{1}H) VTN CP–MAS probehead for solid state experiments, with cross polarization contact time set as 700 μs and 3 s delay between successive scans (total of 16,384). All other NMR experiments were performed using a BB(F)O liquid state probehead with z-gradients. All data processing was carried out using TopSpin 3.2 software and calculations required for diffusion data analysis were carried out using MatLab 2013a software.

The liquid water content determination is based on analysing the first 500 μs of the NMR signal's free induction decay (FID) (Hartley et al. 1994), where the contributions of the protons in solid state and in liquid state can be separated by fitting suitable model functions into the experimental data (see Fig. 1). The methodology for the analysis has been described in detail elsewhere (Topgaard and Söderman 2001, 2002c). The liquid water content is expressed as mass of water ($m_{liqWater}$) divided by mass of pulp (m_{pulp}):

$$\frac{m_{liqWater}}{m_{pulp}} = \frac{S_w^0}{S_c^0} \times RSD, \quad (1)$$

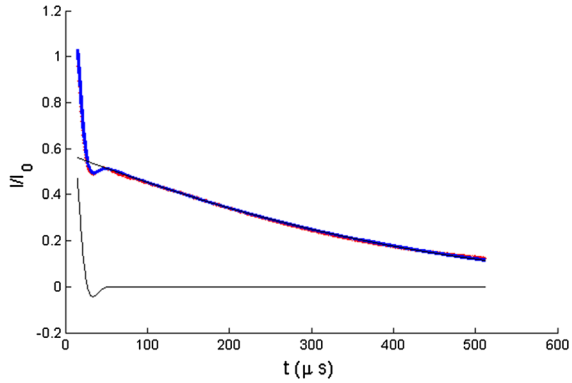

Fig. 1 Quantitation of the amount of liquid water by NMR. The *thin lines* show the model functions that describe the signal from liquid and solid phases. The sum of the liquid and solid phase models is superimposed over the experimental data points

where S_w^0 and S_c^0 are the initial intensities from liquid water and solid material (mainly cellulose) obtained from the fitting. In Eq. (1) *RSD* is the relative spin density, i.e., the ratio of pulp proton spin density to water proton spin density, with a value of 0.56 (Hartley et al. 1994).

The diffusion measurements were carried out at eleven temperatures, starting from 263 K at which the temperature was first allowed to equilibrate for at least 30 min. A 5 min settling time was used in subsequent temperature changes. Five diffusion experiments with diffusion time varying from 30 to 480 ms were performed at each temperature using a stimulated echo (STE) type pulse sequence (Fig. 2). The diffusion data was analysed using the Stejskall–Tanner equation (Stejskal and Tanner 1965), with a correction term that takes into account the anisotropy of water diffusion inside fiber wall, and the effect of cross relaxation of the longitudinal magnetization, as described in the works by Topgaard and Söderman (2002b, c).

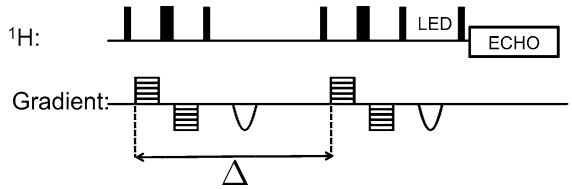

Fig. 2 A pulse sequence for stimulated echo (STE) type diffusion experiment with bipolar gradients and longitudinal eddy current delay (LED). *Δ* marks the diffusion time

The GS experiments were performed by following the method described by Topgaard and Söderman (2002c), and the experimental data were analysed by performing a global fit of a function

$$M_{liq}(\tau_1,\tau_2) = M_{liq}^{eq}\left\{1 + c_1(\tau_1)e^{-R_1\tau_2} + c_2(\tau_1)e^{-R_2\tau_2}\right\} \quad (2)$$

into the data. In Eq. (2) M_{liq}^{eq} is the equilibrium value for liquid magnetization, τ_i are experimentally set delays in the NMR pulse sequence, R_i are functions of cross relaxation rate constants, and c_i are also functions of τ_1. An example of the analysis is shown in Fig. 3. The output from GS experiment is a set of parameters required for diffusion data analysis, including the magnetization cross relaxation rate constant from liquid phase to solid phase (k_{liq}).

The average pore size at the micrometer size scale was calculated from the diffusion results using equation (Valiullin and Skirda 2001)

$$D_a(t_\Delta) = D_\infty + \frac{D_0 - D_\infty}{D_0}\frac{\langle a^2\rangle}{2dt_\Delta} \quad (3)$$

that relates the dependence of the observed apparent diffusion coefficient D_a on diffusion time t_Δ. In Eq. (3) d is the dimensionality of the system (for randomly oriented fibers $d = 3$), D_∞ is the limiting value for apparent diffusion coefficient at long diffusion time, and $\langle a^2\rangle$ is the average squared pore diameter. The long-range connectivity of the pore network is described by its tortuosity α, defined as (Latour et al. 1995; Stallmach and Kärger 1999)

$$\frac{1}{\alpha} = \frac{D_\infty}{D_0}. \quad (4)$$

D_0 in Eqs. (3) and (4) is the self-diffusion coefficient for free diffusion, and it was calculated for each measurement temperature using data given in work by Price et al. (1999).

The diffusion data obtained here provides information only from micrometer size scale pores. By combining fiber saturation point (FSP) values obtained by solute exclusion technique with dextran as molecular probe (Blomstedt et al. 2010) with the data obtained from solid state NMR measurements it is possible to get an estimate for average pore size in nanometer size scale (Larsson et al. 2013). The signal from carbon site C4 was analysed as described by Larsson et al. (1997) and Wickholm et al. (1998), using two Lorentzian functions and one Gaussian function to model crystalline and para-crystalline signals, and three Gaussian functions for modeling the non-crystalline signal region (Fig. 4). Results obtained from the peak fitting were then used to calculate the average lateral cellulose fibril aggregate dimension (LFAD), and the average pore size following the method given by Larsson et al. (2013). With the assumption of a square cross sectional cellulose

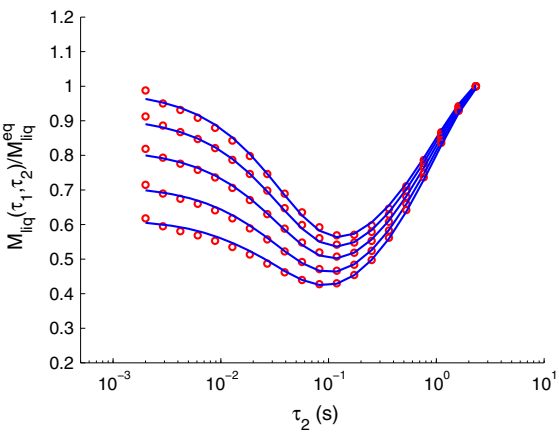

Fig. 3 An analysis of a Goldman–Shen experiment. *Dots* are experimental data points, the *curves* are the result of global fit into the dataset. Each *curve* represents a single τ_1 value, with τ_1 increasing from *top to bottom*

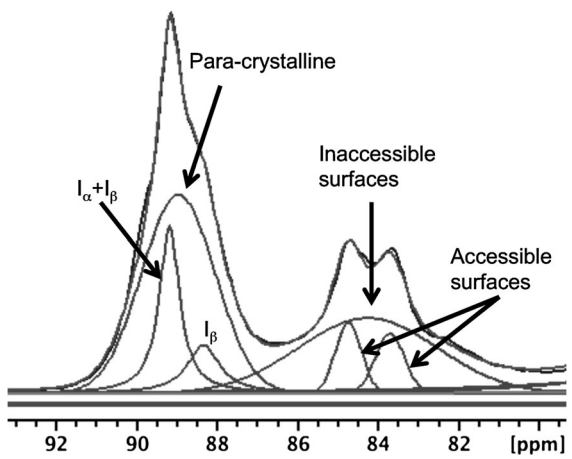

Fig. 4 Deconvolution of C4 signal region in solid state NMR spectrum. The assignments of the fit components are those given by Larsson et al. (1997). The function representing I_α was excluded from the model in order to improve the stability of the fitting procedure

fibril aggregate, the specific surface area σ can be expressed as

$$\sigma = \frac{4}{l\rho_{cel}}, \tag{5}$$

where ρ_{cel} is the density of cellulose and l is the length of the side of the aggregate (i.e., LFAD) obtained from solid state NMR measurement. The fiber saturation point (FSP, mass of water/mass of solids) is given by

$$FSP = d\sigma\rho_{liquid}, \tag{6}$$

where d is the thickness of the liquid layer (uniformly covering the solid surfaces) and ρ_{liquid} is the density of the pore-filling liquid. For water ρ_{liquid} equals 1000 kg m^{-3}. The average pore size is then obtained as twice the liquid layer thickness:

$$\langle a \rangle \equiv 2d = l \times \frac{FSP}{2}\frac{\rho_{cel}}{\rho_{liquid}}. \tag{7}$$

FSP measurements were based on a solvent exclusion technique using a dextran probe molecule (hydrodynamic diameter 54 nm), and is described in work by Grönqvist et al. (2014).

Results and discussion

The complexity of the wood pulp cell wall makes its characterization a challenging task. The experimental methods applied in this work were chosen so that they gather data from different size scales, and thus from different structures in the fiber wall. WAXS and solid state ^{13}C CP–MAS NMR spectroscopy were used to obtain information on cellulose crystallinity and elementary fibril size, whereas microfibrillar aggregation in wet samples was examined with SAXS. An estimation for average pore size at size scale of few tens of nanometers was obtained using solid state NMR in combination with FSP. At the other end, the purpose of NMR diffusometry was to see whether the pretreatments have any effect on the pore network at micrometer size scale. The amount of NFW may be seen as a measure for area of water accessible cellulose fibril surfaces, and the data from GS experiment that was used in calculating the apparent diffusion coefficients can also provide information about level of interaction between the species involved in cross relaxation. Increase in cellulose–water interfaces should lead to enhanced cross relaxation rate, seen as an increased value of the rate constant describing the process. However, it should be kept in mind that due to the structural dispersity of the wood pulp cell wall the obtained average values from each experimental approach should be used only for comparisonal purposes between the samples.

Solid state NMR

The solid state ^{13}C CP–MAS spectra for studied pulp samples are shown in Fig. 5. There are only minor visible differences between the spectra, mostly in the fine structure of C1 and C4 signals that is slightly more prominent for M300, M300ELD, and M300EHD. The crystallinities and lateral fibril dimensions (LFD) obtained by deconvolution of C4 signal are given in Table 2. It can be seen that there are no changes within experimental error in crystallinity or fibril size caused neither by mechanical treatment nor the enzymatic treatment. The average nanometer scale pore diameters $\langle a \rangle_{nm}$ based on solid state NMR results and FSP data are given in Table 3. It can be seen that $\langle a \rangle_{nm}$ is almost doubled after the shortest mechanical treatment, from 7.6 ± 0.4 to 14.8 ± 0.6 nm. The prolonged mechanical treatment and subsequent enzymatic treatment do not affect the pore size within experimental error. It should be noted though that the hydrothermal step that was used to stop the enzyme reaction may promote cellulose fibril aggregation and thus affect the calculated pore sizes. Larsson et al. (2013) obtained an average pore size of 11.9 ± 0.8 nm

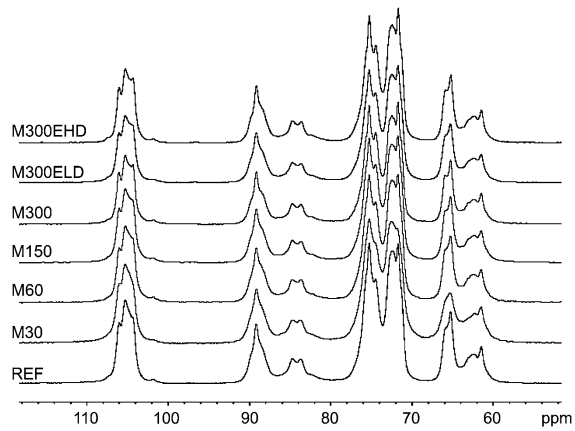

Fig. 5 Solid state ^{13}C CP–MAS NMR spectra of reference pulp and pretreated samples

Table 2 Crystallinities (C) and lateral fibril dimensions (LFD) as determined from solid state NMR data, and distances (d) between microfibrils determined from the SAXS intensities

Sample	C (%)	LFD (nm)	d (nm)
REF	61	5.1	7.5
M30	62	5.1	8.3
M60	60	4.9	8.6
M150	61	5.0	8.9
M300	61	5.1	9.1
M300ELD	63	5.3	10.3
M300EHD	62	5.1	11.1

Table 3 Average nanometer scale pore sizes $\langle a \rangle_{nm}$ based on solid state NMR and FSP results

Sample	*FSP* (g/g)	$\langle a \rangle_{nm}$ (nm)
REF	0.53	7.6 ± 0.4
M30	0.75	14.8 ± 0.6
M300	0.82	15.0 ± 0.6
M300ELD	1.05	15.8 ± 0.8

The uncertainties (one standard error) are based on estimating a one nanometer precision for calculated fibril aggregate size

for never-dried Domsjö dissolving pulp, and 8.0 nm with BET-method in dry state after liquid exchange. Our value for REF agrees better with their dry-state result, which indicates that the pore system in REF is only partially recovered from drying.

WAXS: crystallinity and crystal size

The crystallinity, as calculated from the WAXS intensities (Fig. 6), was 52 % for all mechanically treated samples. This value is slightly lower than the crystallinity values obtained for the same samples with solid-state NMR (60–62 %). The crystal sizes in directions perpendicular to the (1–10), (110), and (200) lattice planes of cellulose I_β were in the ranges 3.6–3.7, 5.0–5.2 and 5.1–5.2 nm, respectively. These values correspond well to the crystal microfibril widths determined with solid-state NMR spectroscopy (4.9–5.3 nm). No changes in crystallinity nor crystal size of cellulose were detected between samples subjected to different times of mechanical treatment.

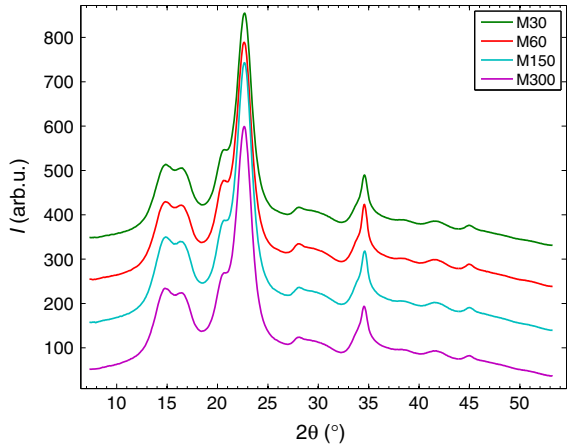

Fig. 6 Wide-angle X-ray scattering (WAXS) intensities of mechanically treated fibers

SAXS: microfibrillar aggregation

The SAXS intensities (Fig. 7a) showed a broad shoulder feature around $q = 0.1$ Å^{-1}, which was seen as a peak in the Kratky plots of the same intensities (Fig. 7b). The location of the peak maximum (q_{max}) in the Kratky plots was used to estimate the centre-to-centre distance between adjacent cellulose microfibrils ($d = 2\pi/q_{max}$). Even though the distance d does not necessarily represent the exact distance between the microfibril centre points, it is expected to correlate with the true average distance and to be therefore suitable for comparisons between similar samples (Fernandes et al. 2011; Testova et al. 2014). As shown by the shift of the peak to smaller q values in Fig. 7b and by the calculated distances d in Table 2, the interfibrillar distance increased slightly with the mechanical treatment: from 7.5 nm for the reference sample (REF) to 8.3 and 9.1 nm for the shortest (M30) and longest (M300) mechanical treatments, respectively. The enzymatic treatment of sample M300 (i.e. samples M300ELD and M300EHD) increased the interfibrillar distance even further and a higher enzyme concentration was observed to enhance this effect (change from 10.3 nm for M300ELD to 11.1 nm for M300EHD). The increase of the interfibrillar distance could be interpreted as a slight opening of the microfibril bundles due to degradation of discontinuity sections caused by the enzyme, or as an enlargement of pores between the microfibrils.

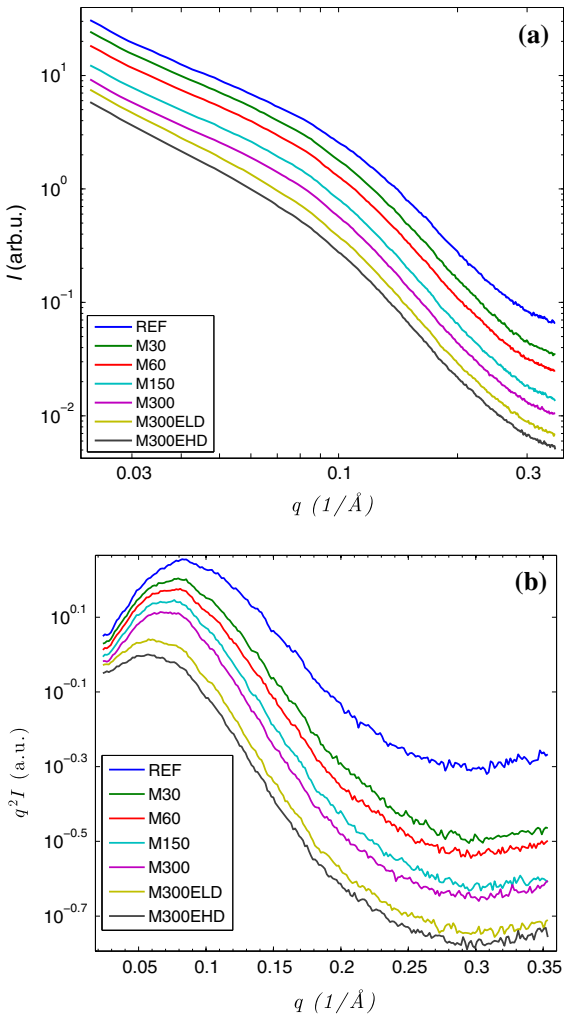

Fig. 7 Small-angle X-ray scattering (SAXS) intensities of wet fibers: **a** on logarithmic scale, **b** on semilogarithmic scale multiplied by q^2 (Kratky plot). Curves in both images have been vertically scaled for clarity

Pore structure from diffusion experiments

The freezing point depression for a liquid confined inside porous material is according to Gibbs–Thomson equation inversely proportional to the pore size (Petrov and Furó 2009). The constant of proportionality for water is ~ 30 nmK. This means that at 272 K water inside pores with diameter over 30 nm is frozen, and at 263 K the limiting pore size for sustaining water in a liquid state becomes 3 nm. According to Topgaard and Söderman (2002c) there exists a thin water layer that remains in liquid state at the fibril surfaces, regardless of the pore size. There exists also

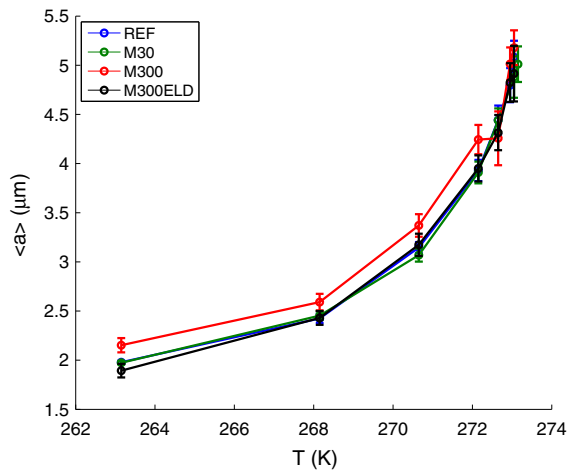

Fig. 8 Average pore size $\langle a \rangle_{\mu m}$ at different temperatures. Lines are for visual clarity

nanometer size scale cavities in the interfibrillar space where water may remain in liquid state. Topgaard and Söderman (2002c) also showed that even at 249 K there exists water molecules in wood pulp fibers that exhibit diffusive motion along these structures over distances at micrometer length scale during 0.1 s diffusion time. In this work these structures that are capable of sustaining liquid water, and that show enough connectivity for making the diffusion of water possible over a micrometer length scale, are referred as micrometer size scale pores. The average pore size $\langle a \rangle_{\mu m}$, as calculated from the diffusion data using Eq. (3), is the dimension along the fiber length axis for the porous network. Figure 8 shows the values for $\langle a \rangle_{\mu m}$ obtained at different measuring temperatures for the pulp samples studied in this work. In lower temperatures the amount of frozen nanometer scale pores increases and the diffusion of water is slowed down. This is seen in the Fig. 8 as lower average pore size. Comparing the $\langle a \rangle_{\mu m}$ values between REF, M30, and M300ELD it can be seen that they do not differ within experimental error. It is therefore to be concluded that the pretreatments do not cause any notable changes on the average pore size in micrometer size scale within the precision of the measurement.

As the ice melts inside the pores the tortuosity decreases, as seen in Fig. 9. At lowest temperature the ice present in pores evidently alters the connectivity of the pore network, but does not completely isolate

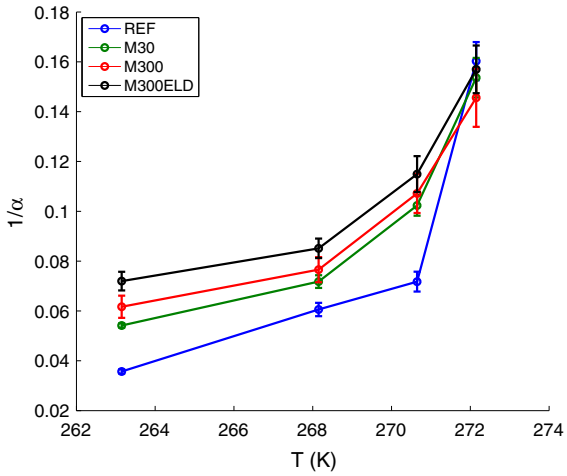

Fig. 9 Inverse of α as observed at different temperatures. The observed increase with increasing temperature is due to melting of ice

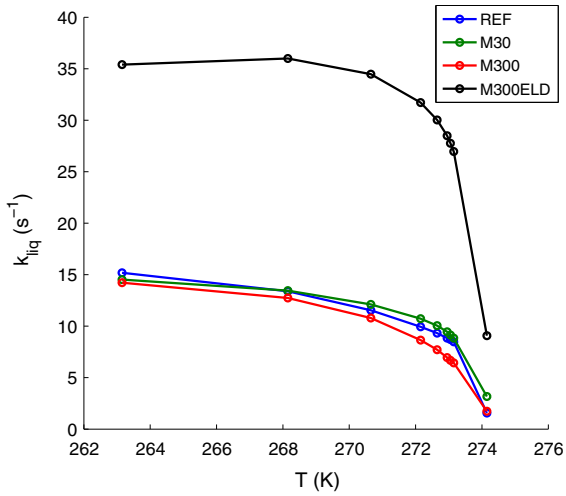

Fig. 10 Magnetization cross relaxation rate constants from liquid phase to solid observed at different measurement temperatures

pores as can be seen from the non-zero value of D_∞. The uncertainty in $\frac{1}{\alpha}$ values becomes more severe when approaching the bulk melting temperature, but at 263 K the order of the samples in terms of higher tortuosity is REF $>$ M30 $>$ M300 $>$ M300ELD. This suggests that mechanical treatment causes an increase in the connections between micrometer scale pores, and subsequent enzymatic hydrolysis enhances this effect. It should be noted, however, that the uncertainties calculated here for the inverse tortuosity and micrometer scale pore sizes are based purely on the calculation of the numerical fit. They do not take into account the natural variation in pulp, and therefore the true uncertainties in these results may be larger than those presented in the figures. It is also apparent that formation of ice inside the pores has an impact to the pore structure and the water diffusion. Therefore, the value of $\frac{1}{\alpha}$ represents the true tortuosity of the fiber only at relatively close to bulk melting temperature of water, when ice formation does not create additional blockages. The alternative approach for detecting diffusion inside the fiber wall would require reducing the moisture content of the fiber, and this could also alter the pore structure.

Cross relaxation rate constants

Figure 10 shows magnetization cross relaxation rate constant from liquid phase to solid phase (k_{liq}) as a function of temperature for studied pulps. The decrease in curves as the temperature approaches 273 K is due to melting of the bulk water, after which the NMR signal mainly originates from water molecules that are not in close contact with pore walls, thus not contributing to cross relaxation. It can be seen that the reference pulp and only mechanically treated pulps have almost equal rate constants. Enzymatic treatment, however, more than doubles the value of k_{liq}. We measured k_{liq} also to several other samples that had gone through enzymatic treatment, and a sample with acidic hydrolysis (data not shown here). An increased level of k_{liq} was observed on pulp sample that was only enzymatically treated (ELD) and with the high-dosage M300EHD, but not for a sample that was acid hydrolyzed to approximately same DP as the enzymatically treated samples. It could be that the observed increase of k_{liq} is associated with the microfibrillar swelling observed by SAXS. As the endoglucanases target the less ordered cellulose regions (Rabinovich et al. 2002; Ibarra et al. 2010), the cellulose fibril bundles gain more freedom to swell and this leads to an increase in solvent accessible sites, seen as an increase in cross relaxation rate. There has been a lack of suitable method for quantifying the reactivity of pulp fibers (Engström et al. 2006). Further investigations are needed to study whether the magnetization cross relaxation would be a suitable measure for pulp reactivity in general.

Amount of nonfreezing water

There is a clear increase in nonfreezing water (NFW) content due to pretreatments as can be seen in Fig 11. The amount of NFW triples when comparing REF and M300, from 0.10 to 0.32 (values at 263 K). Due to our instrumental setup we were not able to carry out the measurements below 263 K. Topgaard and Söderman (2002c) found that the quantity of nonfreezing water for pulp remains essentially constant below 268 K, therefore we assume that also in the case of our samples the amount of NFW observed at 263 K does not change significantly if the temperature was lowered further.

Values obtained here for NFW content in the case of pretreated pulps are in agreement with that observed by Topgaard and Söderman (2002c), but the REF pulp deviates from the other samples notably. This could be explained by the only partial re-swelling and opening of the pores after the drying. The 30 min mechanical treatment clearly increases the amount of NFW, to 0.35 (at 263 K). Apparently the mechanical treatment is more capable of breaking coalesced fibrillar structures that plain re-wetting is, thus increasing water accessible fibril surfaces. On the other hand, prolonged mechanical treatment causes a slight decrease in NFW content. It has been earlier observed that mechanical treatment causes macropores to close (Joutsimo and Robertsén 2005), which could be seen here as the decrease of NFW content.

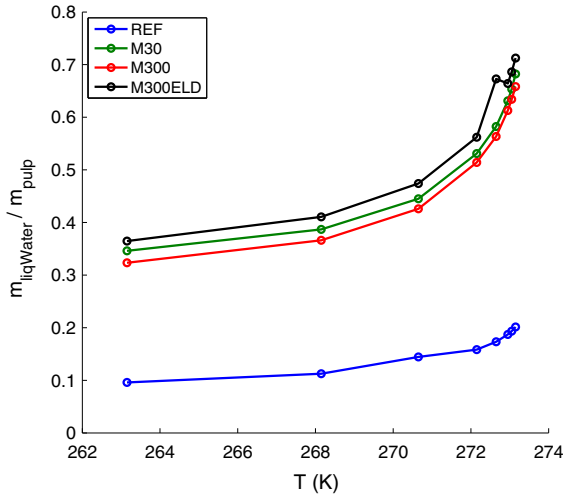

Fig. 11 Amount of nonfreezing water in the studied samples

Considering the large difference in cross relaxation rate constants between M300ELD and rest of the studied pulps, it was expected that similar differences would have been also observed in NFW measurements. According to Topgaard and Söderman (2002c) NFW exists as a thin (about 1 nm) layer on the cellulose fibril surfaces. It would therefore be expected that the increase of water accessible sites, as suggested by the increase in k_{liq}, would also lead to an increased NFW content. M300ELD does indeed have the highest NFW content, but the difference to other pretreated samples is not as large as the increase in cross relaxation rate constant would imply. The modest increase in NFW content in the case of M300ELD could be explained by a slight largening of the nanometer sized pores. This would lead to increase of freezing water in the pore system, thus partially compensating the effect of increasing surface area on the amount of NFW.

Conclusions

We have characterized the effects of mechanical and subsequent enzymatic pretreatments on softwood pulp fiber wall structure by NMR spectroscopic and X-ray scattering methods. According to the WAXS results, the duration of the mechanical treatment did not affect the cellulose crystal size nor the crystallinity of the samples. The same result was also observed with solid state NMR spectroscopy. Based on the SAXS results obtained from samples without drying, the microfibril bundles were slightly loosened during the mechanical treatment and the loosening effect was enhanced by the enzymatic treatment, with a greater effect observed with higher enzyme concentration. The long range connectivity of the pore network at micrometer size scale appeared to be increasing with mechanical treatment time and subsequent enzymatic treatment. There was a major difference between magnetization cross relaxation rate constants for pulps that were enzymatically hydrolyzed compared to those that had only a mechanical pretreatment. This could be related to the increase in interfibrillar spacing that was observed by SAXS. The average macropore size was observed to increase due to mechanical treatment, but prolonged treatment or subsequent enzymatic treatment did not increase the pore size any further within experimental error.

Acknowledgments Finnish Bioeconomy Cluster (FIBIC) FuBio Cellulose program and the Finnish Funding Agency for Innovation (TEKES) are acknowledged for the financial support.

References

Ambjörnsson HA, Östberg L, Schenzel K, Larsson PT, Germgård U (2013) Enzyme pretreatment of dissolving pulp as a way to improve the following dissolution in NaOH/ZnO. Holzforschung 68(4):385–391

Andreasson B, Forsström J, Wågberg L (2003) The porous structure of pulp fibres with different yields and its influence on paper strength. Cellulose 10(2):111–123

Bailey MJ, Biely P, Poutanen K (1992) Interlaboratory testing of methods for assay of xylanase activity. J Biotechnol 23(3):257–270

Blomstedt M, Asikainen J, Lähdeniemi A, Ylönen T, Paltakari J, Hakala TK (2010) Effect of xylanase treatment on dewatering properties of birch kraft pulp. BioResources 5(2):1164–1177

Chunilall V, Bush T, Larsson PT, Iversen T, Kindness A (2010) A CP/MAS 13C-NMR study of cellulose fibril aggregation in eucalyptus dissolving pulps during drying and the correlation between aggregate dimensions and chemical reactivity. Holzforschung 64(6):693–698

Cuissinat C, Navard P (2006) Swelling and dissolution of cellulose part II: free floating cotton and wood fibres in NaOH–Water-additives systems. Macromol Symp 244(1):19–30

Engström AC, Ek M, Henriksson G (2006) Improved accessibility and reactivity of dissolving pulp for the viscose process: pretreatment with monocomponent endoglucanase. Biomacromolecules 7(6):2027–2031

Fahlén J, Salmén L (2003) Cross-sectional structure of the secondary wall of wood fibers as affected by processing. J Mater Sci 38(1):119–126

Fahlén J, Salmén L (2005) Pore and matrix distribution in the fiber wall revealed by atomic force microscopy and image analysis. Biomacromolecules 6(1):433–438 pMID: 15638549

Fernandes AN, Thomas LH, Altaner CM, Callow P, Forsyth VT, Apperley DC, Kennedy CJ, Jarvis MC (2011) Nanostructure of cellulose microfibrils in spruce wood. Proc Natl Acad Sci 108(47):E1195–E1203

Goldman M, Shen L (1966) Spin–spin relaxation in LaF_3. Phys Rev 144:321–331

Grönqvist S, Hakala T, Kamppuri T, Vehviläinen M, Hänninen T, Liitiä T, Maloney T, Suurnäkki A (2014) Fibre porosity development of dissolving pulp during mechanical and enzymatic processing. Cellulose 21(5):3667–3676

Hartley I, Kamke FA, Peemoeller H (1994) Absolute moisture content determination of aspen wood below the fiber saturation point using pulsed NMR. Holzforschung 48:474–479

Hult EL, Larsson P, Iversen T (2001) Cellulose fibril aggregation—an inherent property of kraft pulps. Polymer 42(8):3309–3314

Ibarra D, Köpcke V, Ek M (2010) Behavior of different monocomponent endoglucanases on the accessibility and reactivity of dissolving-grade pulps for viscose process. Enzyme Microb Technol 47(7):355–362

IUPAC (International Union of Pure and Applied Chemistry) (1987) Measurement of cellulase activities. Pure Appl Chem 59(2):257–268

Johnson C Jr (1999) Diffusion ordered nuclear magnetic resonance spectroscopy: principles and applications. Prog Nucl Magn Reson Spectrosc 34(3):203–256

Joutsimo O, Robertsén L (2005) The effect of mechanical treatment on softwood kraft pulp fibers. Fiber wall. Pap Timber 87:41–45

Kihlman M, Wallberg O, Stigsson L, Germgård U (2011) Dissolution of dissolving pulp in alkaline solvents after steam explosion pretreatments. Holzforschung 65(4):613–617

Larsson PT, Wickholm K, Iversen T (1997) A CP/MAS ^{13}C NMR investigation of molecular ordering in celluloses. Carbohydr Res 302(1–2):19–25

Larsson PT, Svensson A, Wågberg L (2013) A new, robust method for measuring average fibre wall pore sizes in cellulose I rich plant fibre walls. Cellulose 20(2):623–631

Latour L, Kleinberg R, Mitra P, Sotak C (1995) Pore-size distributions and tortuosity in heterogeneous porous media. J Magn Reson Ser A 112(1):83–91

Lowry OH, Rosebrough NJ, Farr AL, Randall RJ (1951) Protein measurement with the folin phenol reagent. J Biol Chem 193(1):265–275

Maloney TC, Paulapuro H, Stenius P (1998) Hydration and swelling of pulp fibers measured with differential scanning calorimetry. Nord Pulp Pap Res J 13(1):31–36

Maloney TC, Paulapuro H (1999) The formation of pores in the cell wall. J Pulp Pap Sci 25(12):430–436

Moigne N, Navard P (2010) Dissolution mechanisms of wood cellulose fibres in NaOH–water. Cellulose 17(1):31–45

Moigne NL, Jardeby K, Navard P (2010) Structural changes and alkaline solubility of wood cellulose fibers after enzymatic peeling treatment. Carbohydr Polym 79(2):325–332

Östlund Å, Köhnke T, Nordstierna L, Nydén M (2010) NMR cryoporometry to study the fiber wall structure and the effect of drying. Cellulose 17(2):321–328

Parviainen H, Parviainen A, Virtanen T, Kilpeläinen I, Ahvenainen P, Serimaa R, Grönqvist S, Maloney T, Maunu SL (2014) Dissolution enthalpies of cellulose in ionic liquids. Carbohydr Polym 113:67–76

Penttilä P, Kilpeläinen P, Tolonen L, Suuronen JP, Sixta H, Willför S, Serimaa R (2013) Effects of pressurized hot water extraction on the nanoscale structure of birch sawdust. Cellulose 20(5):2335–2347

Persson PV, Hafrén J, Fogden A, Daniel G, Iversen T (2004) Silica nanocasts of wood fibers: a study of cell-wall accessibility and structure. Biomacromolecules 5(3):1097–1101

Petrov OV, Furó I (2009) NMR cryoporometry: principles, applications and potential. Prog Nucl Magn Reson Spectrosc 54(2):97–122

Pönni R, Vuorinen T, Kontturi E (2012) Proposed nano-scale coalescence of cellulose in chemical pulp fibers during technical treatments. BioResources 7(4):6077–6108

Price WS, Ide H, Arata Y (1999) Self-diffusion of supercooled water to 238 K using PGSE NMR diffusion measurements. J Phys Chem A 103(4):448–450

Rabinovich M, Melnick M, Bolobova A (2002) The structure and mechanism of action of cellulolytic enzymes. Biochemistry (Moscow) 67(8):850–871

Stallmach F, Kärger J (1999) The potentials of pulsed field gradient NMR for investigation of porous media. Adsorption 5(2):117–133

Stejskal EO, Tanner JE (1965) Spin diffusion measurements: spin echoes in the presence of a time dependent field gradient. J Chem Phys 42(1):288–292

Testova L, Borrega M, Tolonen LK, Penttilä PA, Serimaa R, Larsson PT, Sixta H (2014) Dissolving-grade birch pulps produced under various prehydrolysis intensities: quality, structure and applications. Cellulose 21(3):2007–2021

Topgaard D, Söderman O (2001) Diffusion of water absorbed in cellulose fibers studied with ^{1}H-NMR. Langmuir 17(9):2694–2702

Topgaard D, Söderman O (2002a) Changes of cellulose fiber wall structure during drying investigated using NMR self-diffusion and relaxation experiments. Cellulose 9(2):139–147

Topgaard D, Söderman O (2002b) Self-diffusion in two- and three-dimensional powders of anisotropic domains: an NMR study of the diffusion of water in cellulose and starch. J Phys Chem B 106(46):11,887–11,892

Topgaard D, Söderman O (2002c) Self-diffusion of nonfreezing water in porous carbohydrate polymer systems studied with nuclear magnetic resonance. Biophys J 83(6):3596–3606

Valiullin R, Skirda V (2001) Time dependent self-diffusion coefficient of molecules in porous media. J Chem Phys 114(1):452–458

Vehviläinen M, Nousiainen P, Kamppuri T, Järventausta M (2009) A method for dissolving cellulose and a cellulosic product obtained from a solution comprising dissolved cellulose. EP Patent App. EP20,080,397,510

Wang X, Maloney TC, Paulapuro H (2006) Improving the properties of never-dried chemical pulp by pressing before refining. Nord Pulp Pap Res J 21(1):135–139

Wickholm K, Larsson PT, Iversen T (1998) Assignment of non-crystalline forms in cellulose I by CP/MAS ^{13}C NMR spectroscopy. Carbohydr Res 312(3):123–129

Woessner DE (1963) N.M.R. spin-echo self-diffusion measurements on fluids undergoing restricted diffusion. J Phys Chem 67(6):1365–1367

Zhu S, Wu Y, Chen Q, Yu Z, Wang C, Jin S, Ding Y, Wu G (2006) Dissolution of cellulose with ionic liquids and its application: a mini-review. Green Chem 8:325–327